Loss of phosphatidylinositol 4-kinase 2α activity causes late onset degeneration of spinal cord axons

J. Paul Simons[a,b,1,2], Raya Al-Shawi[a,b,2], Shane Minogue[a,b], Mark G. Waugh[a], Claudia Wiedemann[a,3], Stylianos Evangelou[a], Andrzej Loesch[a], Talvinder S. Sihra[c], Rosalind King[d], Thomas T. Warner[d], and J. Justin Hsuan[a,b,1]

[a]Division of Medicine, [b]Royal Free Centre for Biomedical Science, and [d]Division of Neuroscience, University College London Medical School, University College London, Rowland Hill Street, London NW3 2PF, United Kingdom; and [c]Department of Pharmacology, University College London, Gower Street, London WC1E 6BT, United Kingdom

Edited by Lewis C. Cantley, Harvard Institutes of Medicine, Boston, MA, and approved May 28, 2009 (received for review March 18, 2009)

Phosphoinositide (PI) lipids are intracellular membrane signaling intermediates and effectors produced by localized PI kinase and phosphatase activities. Although many signaling roles of PI kinases have been identified in cultured cell lines, transgenic animal studies have produced unexpected insight into the in vivo functions of specific PI 3- and 5-kinases, but no mammalian PI 4-kinase (PI4K) knockout has previously been reported. Prior studies using cultured cells implicated the PI4K2α isozyme in diverse functions, including receptor signaling, ion channel regulation, endosomal trafficking, and regulated secretion. We now show that despite these important functions, mice lacking PI4K2α kinase activity initially appear normal. However, adult *Pi4k2a*$^{GT/GT}$ animals develop a progressive neurological disease characterized by tremor, limb weakness, urinary incontinence, and premature mortality. Histological analysis of aged *Pi4k2a*$^{GT/GT}$ animals revealed lipofuscin-like deposition and gliosis in the cerebellum, and loss of Purkinje cells. Peripheral nerves are essentially normal, but massive axonal degeneration was found in the spinal cord in both ascending and descending tracts. These results reveal a previously undescribed role for aberrant PI signaling in neurological disease that resembles autosomal recessive hereditary spastic paraplegia.

genetrap | hereditary spastic paraplegia | phosphoinositide | lipofuscin | neurodegeneration

Studies of PI signaling have identified roles in many cell functions, including mitogenesis, endocytosis, secretion, phagocytosis, apoptosis, neurotransmission, and migration. Key to this functional diversity is the differential regulation and localization of PI 3-, 4-, and 5-kinase isozymes. Sequence similarities between the 19 human PI kinase genes define the PI 3-kinase (PI3K), phosphatidylinositol phosphate kinase (PIPK), and type 2 PI4K (PI4K2) families. Recent transgenic studies have produced valuable information on in vivo roles of several PI3K and PIPK isozymes and provided useful models to study human disease and therapeutic intervention (1–5). Here, transgenics are used to address the in vivo function of a mammalian PI4K.

The four mammalian PI4K isozymes differ in expression pattern, biochemical properties, and subcellular localization. PI4K2α, the subject of this work, is expressed in all tissues analyzed and is predominantly located in the Golgi complex and endosomes. PI4K2α kinase activity is implicated in receptor signaling, ion channel regulation, and vesicle trafficking (6). Phosphatidylinositol 4-phosphate (PI4P), generated primarily by either PI4K activity on phosphatidylinositol (PtdIns) or by 5-phosphatase activity on phosphatidylinositol 4,5-bisphosphate (PIP_2), is the most abundant polyphosphoinositide in mammalian cells. Although PI4P has been thought of simply as a precursor of PIP_2, there is now abundant evidence for its own functional importance (6).

Knockout of the single yeast PI4K2 isozyme failed to identify a role for the enzyme activity (7, 8), but revealed instead a nonenzymatic function in late endosome motility (7, 9). PI4K2α RNA interference in cultured mammalian cells established requirements in Wnt signaling (10), vesicle export from the *trans*-Golgi network (TGN) (11, 12), and endosomal trafficking (13, 14). Nonetheless, the physiological or pathophysiological importance in mammals is unknown as no transgenic phenotype or disease has been associated with the *PI4K2a* gene.

We now describe the generation and characterization of mice lacking PI4K2α kinase activity. These mice develop late-onset neurological features that resemble human hereditary spastic paraplegia (HSP) (15), thereby revealing a previously undescribed phenotype for aberrant PI signaling.

Results

Generation of Pi4k2α-Deficient Mice. A search of the Sanger Institute Gene Trap Resource (16) showed 4 murine ES cell lines carrying a *Pi4k2a* gene trap. Based on integration site and cultured cell appearance, we chose line AK0094. Corresponding 5′-RACE PCR data indicated vector integration into intron 2 (Fig. 1*A*), predicting a fusion protein lacking the PI4K2α catalytic domain, comprising PI4K2α amino acid residues 1–212 and the selectable β-geo (LacZ/Neo^r) protein.

Chimaeras were generated with AK0094 cells, and germ-line transmission was obtained. In brain membrane preparations, where PI4K2α provides the majority of measurable PI4K activity (17), we found ≈50% lower activity in heterozygotes than in wild-type mice, confirming the gene-trap target as *Pi4k2a* and the cognate loss of activity. Anticipating homozygous lethality and for endocytosis studies, we isolated primary embryo fibroblasts (PEFs) from *Pi4k2a*$^{+/GT}$ × *Pi4k2a*$^{+/GT}$ crosses. PI4K activities in cultured PEFs fell into 3 groups: The lowest activity group had <5% wild-type activity (attributable to other PI4K isozymes) and were presumed to be gene trap homozygotes. PCR scans using genomic DNA from this group confirmed homozygous disruption of intron 2 between bases 2,734–3,385.

Viability of *Pi4k2a*$^{GT/GT}$ mice was normal, as live animals were obtained from heterozygote crosses at ≈25% (χ^2 = 2.303, 1df; P = 0.3162; n = 390). PI4K assays of *Pi4k2a*$^{GT/GT}$ brain membranes yielded minimal activity (<5%), and Western blotting confirmed the absence of native PI4K2α (Fig. 1 *B* and *C*).

Author contributions: J.P.S., R.A.-S., and J.J.H. designed research; J.P.S., R.A.-S., S.M., M.G.W., C.W., S.E., A.L., T.S.S., and R.K. performed research; C.W. contributed new reagents/analytic tools; J.P.S., R.A.-S., T.S.S., T.T.W., and J.J.H. analyzed data; and J.P.S. and J.J.H. wrote the paper.

The authors declare no conflict of interest.

This article is a PNAS Direct Submission.

[1]To whom correspondence may be addressed. E-mail: simons@medsch.ucl.ac.uk or j.hsuan@medsch.ucl.ac.uk.

[2]J.P.S. and R.A.-S. contributed equally to this work.

[3]Present address: Nature Reviews Neuroscience, 4 Crinan Street, London N1 9XW, United Kingdom.

This article contains supporting information online at www.pnas.org/cgi/content/full/0903011106/DCSupplemental.

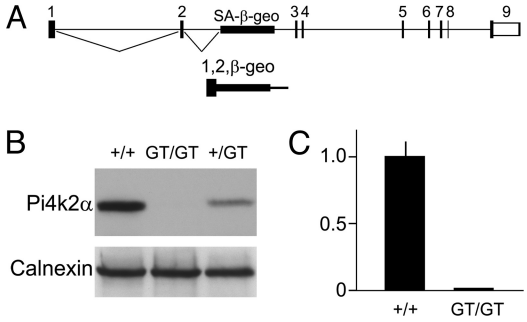

Fig. 1. Gene trap and absence of PI4K2α protein and activity in *Pi4k2a*$^{GT/GT}$ mice. (*A*) The gene-trap allele contains the inserted splice acceptor-β-geo (SA-β-geo) cassette in the second intron of the *Pi4k2a* gene. The predicted transcript contains exons 1 and 2 of *Pi4k2a* followed by β-geo. (*B*) Anti-PI4K2α Western blots of brain protein extracts from *Pi4k2a*$^{GT/GT}$ (GT/GT), *Pi4k2a*$^{+/GT}$ (+/GT), and *Pi4k2a*$^{+/+}$ (+/+) mice; anti-calnexin blots were used as a loading control. (*C*) PI4K activity assays of brain membrane proteins from *Pi4k2a*$^{GT/GT}$ (GT/GT) and *Pi4k2a*$^{+/+}$ (+/+) mice.

Endosomal Trafficking. We have shown that siRNA or mAb-mediated knockdown of PI4K2α leads to mistrafficking of internalized EGF (13). We therefore incubated PEFs with labeled EGF and followed endocytosis by using confocal microscopy. The patterns of EGF fluorescence in *Pi4k2a*$^{GT/GT}$ and *Pi4k2a*$^{+/+}$cells were indistinguishable. No differences were found in transferrin internalization (18) or Golgi integrity (12) as revealed by gm130 immunostaining.

***Pi4k2a* Expression.** We took advantage of the β-gal activity of the gene-trap fusion protein to identify sites of *Pi4k2a* gene expression. Although expression was too low to permit analysis at the cellular level by X-gal staining, whole midgestation *Pi4k2a*$^{+/GT}$ embryos showed widespread low-level expression (Fig. 2*B*) with signal concentrated in the first branchial arch and fore-, mid-, and hindbrain. Liver, skeletal muscle, neural tube, and skin appeared weak to negative. No staining of wild-type embryos was observed under identical conditions (Fig. 2*A*). Stained vibratome sections of adult brain revealed highest expression in the cerebellar molecular layer (ML). On prolonged incubation, stain was observed in most brain regions, including the cortex, hippocampus, midbrain nuclei, and striatum. White matter and the granule cell layer (GCL) of the cerebellum were negative (Fig. 2 *C–E*).

Expression in the brain was analyzed by immunostaining rat tissue with a rat PI4K2α-specific mAb. This analysis revealed abundant signal in neurons and astrocytes. In the cerebellum, Purkinje cell bodies exhibited very strong signal, with weaker signal in proximal dendrites; in fresh-frozen tissue, abundant staining of Bergmann glia was evident, as was staining of astrocytes within the GCL (Fig. 2*F*). GCL neurons were negative (Fig. 2*F*), but neurons of cerebellar nuclei were strongly positive (Fig. S1*A*). In other brain regions, including the cerebral cortex, all neurons expressed PI4K2α (Fig. 2 *G* and *H*). There is no published histological analysis of PI4K2α expression for comparison nor a PI4K2α entry in the Protein Atlas (www.proteinatlas.org). However, the rat brain results are consistent with the pattern of X-gal stain in *Pi4k2a*$^{+/GT}$ mice and with mouse brain in situ hybridization data (www.brain-map.org). Abundant expression was also observed in dorsal root ganglion (DRG) neurons and in all neurons in the basal and alar plates of the spinal cord (Fig. S1 *B*, *D*, and *F*).

Phenotype of *Pi4k2a*$^{GT/GT}$ Mice. Young *Pi4k2a*$^{GT/GT}$ mice had no overtly abnormal phenotype, but older mice developed several abnormalities. The first phenotypic sign was incontinence, followed by a high-frequency nodding tremor that was absent in resting mice (Fig. 3 *A–C* and Movie S1). The earliest onset of tremor was at 4 months of age, but typically appeared at 6–8 months in males and 10–12 months in females. Subsequently, these mice developed a spastic gait (Movie S2), initially with hind-limb weakness that progressed to forelimbs, with earlier onset in males. At later stages resting mice failed to support their heads (Fig. 3*A*). Normal mice spread their hind-limbs when lifted by the tail, whereas in common with many neurodegenerative mutants, *Pi4k2a*$^{GT/GT}$ mice clasped their hind-limbs when suspended (Fig. 3*D* and Movie S3). Severity of the phenotype increased with age with affected mice typically becoming weak and losing weight at 10–12 months of age. This decline was ameliorated by a wet diet, suggesting that weight loss is due in part to feeding problems. Affected mice maintained a robust righting reflex at all stages showing maintenance of vestibular

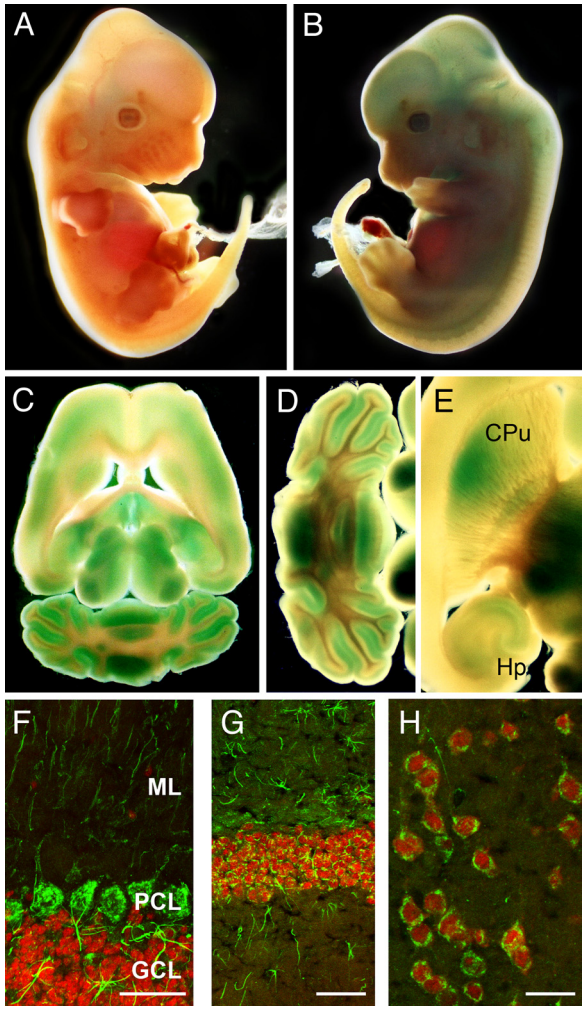

Fig. 2. Expression of PI4K2α. (*A–E*) X-gal-stained whole-mount E12.5 embryos (*A*, wild-type; *B*, *Pi4k2a*$^{+/GT}$) and adult brain sections (C–E) arising from expression of β-geo protein from the *Pi4k2a* promoter. (C) Blue stain is evident in cerebral cortex, cerebellum, and thalamus; (*D*) in the cerebellum, stain is confined to the molecular layer; (*E*) stain observed in the hippocampus (Hp) and Striatum (CPu). (*F–H*) Immunofluorescent localization of PI4K2α (green) in rat brain sections, counterstained for NeuN (red). (*F*) In the cerebellum, PI4K2α is expressed in Bergman glia in the molecular layer (ML) and the large Purkinje neurons of the Purkinje cell layer (PCL). PI4K2α expression in the granular cell layer (GCL) is observed in astrocytes, but not neurons. (*G*) PI4K2α expression in granule cells of the hippocampal dentate gyrus and astrocytes. (*H*) PI4K2α expression in motor cortex; note that every NeuN-positive neuron is also PI4K2α-positive. (Scale bars: *F* and *G*, 50 μm; *H*, 25 μm.)

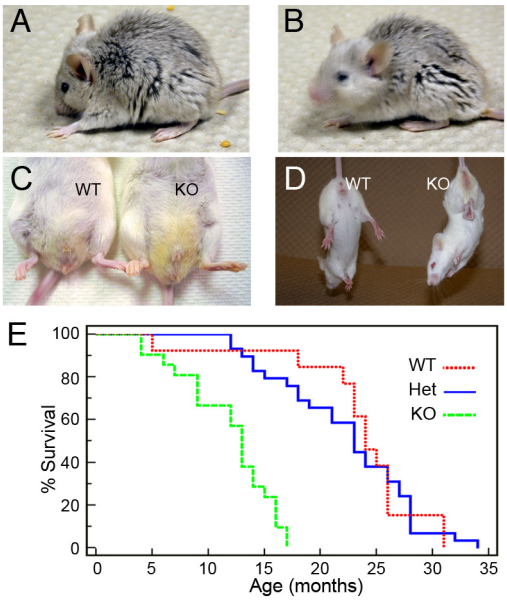

Fig. 3. Phenotype of *Pi4k2a*$^{GT/GT}$ mice. Weakness is evident from the hunched posture of this affected mouse, which had its head resting on the substrate when at rest (*A*). The nodding tremor is absent when affected mice are at rest, but appears when they move (*B*). Exposures were for 0.3 s without flash. (*C*) Urinary incontinence is evident from the stained fur of the *Pi4k2a*$^{GT/GT}$ mouse (KO) compared with an age-matched wild-type mouse (WT). (*D*) Suspended *Pi4k2a*$^{GT/GT}$ mouse (KO) with clasped hind-legs drawn into its abdomen, in contrast to the normal splayed legs of a wild-type mouse (WT). (*E*) Kaplan-Meier survival plot of *Pi4k2a*$^{GT/GT}$ (KO), *Pi4k2a*$^{+/GT}$ (Het), and *Pi4k2a*$^{+/+}$ (WT) mice. Survival of *Pi4k2a*$^{GT/GT}$ mice ($n = 21$) was reduced compared with *Pi4k2a*$^{+/GT}$ ($n = 29$) or *Pi4k2a*$^{+/+}$ ($n = 13$) animals ($P < 0.0001$ for both); survival of *Pi4k2a*$^{+/GT}$ and *Pi4k2a*$^{+/+}$ mice were indistinguishable ($P = 0.945$).

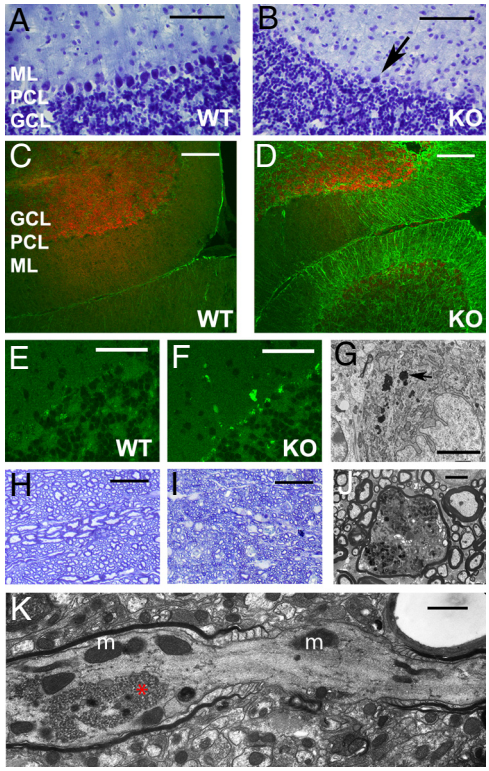

Fig. 4. Neurodegeneration in *Pi4k2a*$^{GT/GT}$ mice. Cerebellar Purkinje cells are lost in affected *Pi4k2a*$^{GT/GT}$ mice; (*A* and *B*) cresyl violet-stained sections of littermate WT and *Pi4k2a*$^{GT/GT}$ (KO) mice. In (*B*) only a single Purkinje cell remains (arrow); areas of Purkinje cell loss are interspersed with normal areas. (*C* and *D*) GFAP immunostaining (green) and propidium iodide counterstain (red) showing the gliosis accompanying Purkinje cell loss (*D*); autofluorescence was suppressed with $CuSO_4$. (*E* and *F*) Autofluorescent material accumulation in Purkinje cells of *Pi4k2a*$^{GT/GT}$ mice compared with WT littermates. (G) The incidence of autofluorescent material correlates with higher amounts of lipofuscin-like deposits (arrow) observed by TEM. (*H–K*) Axon degeneration in *Pi4k2a*$^{GT/GT}$ mice: (*H* and *I*) semithin spinal cord sections reveal extensive axonal degeneration in comparable regions of the lumbar cord of WT (*H*) and *Pi4k2a*$^{GT/GT}$ (*I*) mice. Marked axonal loss and/or reduced caliber in mutant mice is accompanied by numerous swollen axons. (*J* and *K*) TEM of ultrathin spinal cord sections showing swollen axons, whereas myelin sheaths appear normal; (*K*): Swelling adjacent to a node of Ranvier. (m, mitochondria; asterisk, membranous inclusions). (Scale bars: *A–D*, 100 μm; *E* and *F*, 50 μm; *G*, 5 μm; *H*, 25 μm; *J*, 2.5 μm, and *K*, 1 μm.)

and cerebellar functions. Younger affected mice had a normal auditory startle response (aged mice failed to respond irrespective of genotype). *Pi4k2a*$^{GT/GT}$ males are infertile, and females are subfertile. The phenotype is 100% penetrant in homozygotes and invariably fatal (Fig. 3*E*); 24–33-month-old heterozygotes appeared normal ($n = 15$).

Serum Analysis. A broad range of markers was analyzed in samples from age-matched (2–8 months) male and female *Pi4k2a*$^{+/+}$ and *Pi4k2a*$^{GT/GT}$ mice. Levels of alanine aminotransferase, albumin, alkaline phosphatase, bilirubin, protein, urea nitrogen, calcium, cholesterol, creatinine, glucose, phosphorus, triglycerides, chloride, potassium, and sodium showed little to no difference between wild-type and mutant groups, indicating no obvious liver or kidney disease. The levels of aspartate aminotransferase (AST) were moderately higher (two-tailed t test with equal variance, $P < 0.001$) in male (123 ± 23 units/L, $n = 8$) and female (162 ± 26 units/L, $n = 5$) *Pi4k2a*$^{GT/GT}$ compared with male (54 ± 3 units/L, $n = 8$) and female (66 ± 6 units/L, $n = 6$) *Pi4k2a*$^{+/+}$ mice. Four of the 8 male *Pi4k2a*$^{GT/GT}$ mice developed the mutant phenotype only after the sampling period; the levels of AST in these mice were consistently lower than in the affected *Pi4k2a*$^{GT/GT}$ males (range 81–118 units/L and 124–147 units/L, respectively). Creatine kinase assays showed only small differences between homozygous mutant (108 ± 21 units/L, $n = 3$) and wild-type (74 ± 15 units/L, $n = 3$) mice ($P < 0.1$). These data reveal no severe myopathy.

Neurodegeneration. The brains of *Pi4k2a*$^{GT/GT}$ mice showed no gross anatomical defects. Affected animals had reduced numbers of cerebellar Purkinje cells (Fig. 4 *A* and *B*), whereas presymptomatic young adults had normal levels, demonstrating that the Purkinje cell deficiency is not developmental. Loss was patchy, and no *Pi4k2a*$^{GT/GT}$ mouse lacked >25% of these neurons.

CNS injury or neuron loss is typically accompanied by reactive gliosis (astrocyte proliferation). In affected mice, Purkinje cell loss was accompanied by astrocytosis in the GCL and Bergmann gliosis in the ML (Fig. 4 *C* and *D*). No gliosis was consistently observed in any other site in affected mice, although small areas were seen in cerebella of some young, presymptomatic *Pi4k2a*$^{GT/GT}$ mice.

We found distinctly higher autofluorescence in Purkinje cells of *Pi4k2a*$^{GT/GT}$ mice than in controls (Fig. 4 *E* and *F*) with some cells showing very high levels (Fig. 4*F*). Increased autofluorescence was detected across a range of wavelengths in the visible spectrum, consistent with lipofuscin-like deposition (19). In electron micrographs, Purkinje cells of *Pi4k2a*$^{GT/GT}$ mice (Fig. 4*G*) have larger accumulations of lipofuscin-like electron-dense material than age-matched controls. The inclusions were negative for α-synuclein, Tau, and ubiquitin.

The spinal cords of affected mice had axonal defects of both ascending and descending tracts (Fig. 4 *H* and *I* and Fig. S2). There was massive axonal degeneration with almost complete absence of the largest caliber axons and numerous swollen axons (Fig. 4 *I–K*), often containing numerous mitochondria (Fig. 4*K*); the nodal gap was sometimes abnormally wide (Fig. 4*K*). Membrane-derived axonal inclusions were observed (Fig. 4*K*), as were inclusions of glycogen (Fig. S3 *A* and *B*). The presence of macrophages indicated ongoing degeneration (Fig. S3 *C* and *D*). Apart from minor normal age-related demyelination, myelin sheaths (surrounding healthy axons) appeared normal. Neurons in spinal cord gray matter were normal in number and appearance. Peripheral nerves (sciatic, phrenic, and vagus) also appeared normal, although in DRGs we have found inclusion of multivesicular bodies and some axon loss (Fig. S3 *E* and *F*). Skeletal muscles (soleus and plantaris) and the detrusor muscle appeared normal. Nerve conduction studies revealed no differences between sciatic nerves of *Pi4k2a*$^{GT/GT}$ and *Pi4k2a*$^{+/+}$ mice.

Discussion

The survival and development of the mice described here is remarkable given the profound in vitro phenotypes caused by acute PI4K2α knockdown or inhibition. An in vitro requirement for PI4K2α kinase activity is indicated in TGN export by rescue with synthetic PI4P (12) and in endosomal trafficking by inhibition with an enzyme-inhibiting antibody (13). Furthermore, kinase-dead PI4K2α fails to rescue the endosomal phenotype of PI4K2α-deficient cells (14). The absence of an immediately lethal phenotype and the different endocytotic trafficking phenotypes of *Pi4k2a*$^{GT/GT}$ cells and *PI4K2A* siRNA-treated cells (13) indicate functional plasticity of PI4K2α-dependent pathways. We found no compensatory up-regulation of PI4K activity afforded by other PI4K isozymes, and identification of rescue pathways promises to provide valuable information on PI4K2α signaling. Another possibility is that some PI4K2α functions may be contributed by the N-terminal domain, which includes the signature tetracysteine motif that is essential for appropriate membrane interaction (20): In this regard the role played by the yeast PI4K2 homologue LSB6 in endocytic vesicle movement does not seem to require the catalytic domain (7, 8). Whatever the mechanism(s), rescue is incomplete, and in time severe neurological deficits ensue.

In vitro, PI4K2α-generated PI4P appears necessary for membrane recruitment of GGA, AP-1, and AP-3 (11, 12, 14). PI4K2α also interacts directly with AP-3 (21), which mediates axonal transport (22): AP-3A is required to target endosomal cargo to lysosomes in neuronal cell bodies and lipofuscinosis is caused by AP-3 deficiencies in mice and man (23), a possible link to the lipofuscinosis observed in this study. AP-3B is required to target endosomal cargo from the cell body to the axon and synaptic vesicles, a possible link to the defective axonal transport implicated in HSP. AP-3B is also required to generate synaptic vesicles in presynaptic endosomes (22). PI4K2α is the only PI4K isozyme found in synaptic vesicles, which also contain PtdIns (17, 24, 25), and both PI4K2α and AP-3 have been implicated in formation of the reserve pool (26, 27). However, studies based on inhibition of synaptosome function have produced conflicting results concerning a role for PI4K2α in neurotransmitter release (24, 26, 28). Although detailed studies are needed to comprehensively assess synaptic vesicle function, our preliminary studies on synaptosomes from age-matched *Pi4k2a*$^{GT/GT}$ and WT mice revealed attenuated glutamate uptake but no difference in glutamate release.

Pi4k2a$^{GT/GT}$ mice present with features resembling HSP (also known as familial spastic parapesis and Strümpell-Lorrain disease), a diverse group of neurodegenerative disorders characterized by progressive lower-limb spasticity and weakness, often with bladder and proprioceptive involvement (15). Typically, as in our mice, peripheral nerve and muscle involvement are absent. "Complicated HSP" includes additional features such as ataxia and mental retardation. HSP is characterized pathologically by degeneration of long ascending and descending spinal cord axons, as observed in the *Pi4k2a*$^{GT/GT}$ mice. The specificity of the deficits is not explained by selective expression of PI4K2α: We observed no difference in expression between layer 5 neurons of the motor cortex (which project into the corticospinal tract) and other cortical neurons. Preferential dying-back of the longest axons, possibly because of disruption of axonal transport or mitochondrial function (15), explains the selective effects on the legs. Similarly the uniquely complex dendritic arbors of Purkinje neurons may render these cells particularly vulnerable. The lack of gliosis in the motor cortex suggests there was no significant death of upper motor neurons, thus the massive corticospinal tract defects are unlikely to be secondary to cell body loss. The deficits of spinal axons and cerebellar Purkinje cells afford sufficient explanation of the overt phenotype of these mice. Spinal axon degeneration and the absence of peripheral nerve defects show that these mice conform to the definition of HSP.

HSP is very heterogeneous genetically with >40 HSP loci having been mapped in man. Identified HSP genes have diverse cellular activities, although several of these functions converge on axon transport. Paraplegin (*SPG7*) mutations result in mitochondrial dysfunction with secondary axon transport defects (29), and defective axon transport is implicated in several other types of HSP: KIF5a (*SPG10*), spastin (*SPG4*), and atlastin (*SPG3A*) all have roles in microtubule-dependent axonal vesicle transport (15). Inhibition of PI4K activity has indicated a role in retrograde axonal transport (30, 31), and the phenotype of *Pi4k2a*$^{GT/GT}$ mice is consistent with defective axon transport. Because of the importance of the PI system in membrane trafficking, the involvement of PIs in HSP is unsurprising. The effects of PI4K2α-deficiency may result from a direct deficit of PI4P or could result in part from insufficiency of PI4P derivatives; notably PIP_2 is required for axonal mitochondrial transport (32).

The age of onset of symptoms in *Pi4k2a*$^{GT/GT}$ mice is lower in males. In an SPG4 family with an atypical partial duplication of the spastin gene, penetrance is lower and onset is later in females (33); together, these data might indicate a functional interaction between PI4K2α activity and spastin. It has also been reported that estrogen can enhance retrograde axonal transport (34). However, the reasons for the sex difference in *Pi4k2a*$^{GT/GT}$ mice may lie elsewhere.

Previously, only 2 identified HSP genes had a clear link to PI signaling: *ZFYVE26* (*SPG15*) and *ZFYVE27* (*SPG33*). These HSP genes encode proteins containing FYVE domains, although these domains are thought to be specific for PI3P, and there is debate about whether *ZFYVE27* is genuinely an HSP gene (35). Although any functional link between PI4K2α and HSP proteins remains to be identified, it is also feasible that loss of PI4K2α activity defines a new route to HSP. For over half of the HSP loci, the genes in question remain unidentified. Of particular interest are the genes for SPG9 (10q23.3-q24.2) and SPG27 (10q22.1-q24.1), which have yet to be identified and appear to include the *PI4K2A* locus at 10q24. We conclude that *PI4K2A* and genes encoding PI4P-interacting proteins are strong candidates for HSP genes in man.

Materials and Methods

Standard methods used to stain for β-gal activity, for serum analysis, PI4K assays, and Western blotting are included in *SI Text*.

Mice. ES cell lines with *Pi4k2a* gene traps (Sanger Institute Gene Trap Resource) were grown and injected into blastocysts as described (36). Mice carrying the knockout allele were backcrossed onto BALB/c mice (Charles River). Most mice

used were from the 4th generation backcross. Genotyping was done by PCR with primers AGAAAGTATCCATCATGGC and TCTTCGTCCAGATCATCC (*Pi4k2a*^{GT}) and AGAAAGTATCCATCATGGC and TCTTCGTCCAGATCATCC (WT). Mice for analysis were generated from *Pi4k2a*$^{+/GT}$ × *Pi4k2a*$^{+/GT}$ matings. A phenotypic study was based on the SHIRPA primary screen (37). Transmission ratios were analyzed by using the χ^2 test, and survival analysis used the Logrank test (MedCalc). This work was approved by the local Ethics and Welfare Committee and conducted according to the Animals (Scientific Procedures) Act, 1986.

Brain Membrane Preparation. Single mouse brains were disrupted by Dounce homogenization on ice in 10 mM Tris-HCl, 1 mM EDTA, 1 mM EGTA, and 0.25 M sucrose, pH 7.4, containing Complete protease inhibitors (Roche). Homogenates were centrifuged for 5 min at 1,000 × *g* at 4 °C to pellet nuclei and cell debris. Postnuclear supernatants were spun at 20,000 × *g* for 30 min at 4 °C to pellet remaining membranes. After decanting the supernatants, membrane pellets were resuspended in homogenization buffer.

CNS and Peripheral Nerve Histology. Cresyl violet staining was performed on 15-μm brain cryosections. For other histology, mice were perfused with 1% paraformaldehyde, 1% glutaraldehyde, and 1% dextran in Pipes buffer. Tissues were postfixed in 1% OsO_4, dehydrated, and embedded in epoxy resin. Semithin sections for light microscopy were stained with thionin and acridine orange. Ultrathin sections for electron microscopy were stained with uranyl acetate and lead citrate.

Autofluorescence emission spectra of inclusion bodies were recorded from 4% paraformaldehyde fixed, unstained specimens on a Zeiss LSM 510 Meta by excitation at 488 nm by using a Kr-Ar laser.

Immunofluorescence. Mouse and rat tissues were either fresh-frozen or fixed by transcardial perfusion with 4% paraformaldehyde in PBS before cryosectioning at 15 μm. Antibodies were: rabbit anti-Tau (1:500; Dako); rabbit anti-GFAP 1:1,000 (Dako); rabbit anti-ubiquitin at 1:250 (Chemicon); sheep anti-α-synuclein at 1:1,000 and 1:300 (Chemicon); AlexaFluor488-conjugated anti-Neu-N (Chemicon); and 7B4 anti-rat PI4K2α (hybridoma supernatant). Secondary antibodies were goat anti-rabbit AlexaFluor488, goat anti-rabbit AlexaFluor568, goat anti-mouse AlexaFluor488, goat anti-mouse AlexaFluor568 (all used at 1:400; Invitrogen/Molecular Probes), and rabbit anti-sheep secondary antibody at 1:200 (Vector Labs). Autofluorescence was suppressed by treatment with 10 mM $CuSO_4$ in 50 mM NH_4OAc, pH 5.0, for 30 min (38).

PEFs cultured in DMEM/15% FCS were analyzed at passage 2–4. Cells were serum starved and endosomal compartments labeled by incubation for 15 min with Alexa 568 transferrin or EGF conjugates and processed as described (13). Cells were also immunostained with antibodies to gm130 (1:250; BD Biosciences).

ACKNOWLEDGMENTS. We thank Julian Blake for communicating unpublished data; Tim Robson, Samrina Aslam, and Michelle Nourallah for technical assistance; and the Sanger Institute for ES cell lines. We gratefully acknowledge support provided by the Royal Free Hampstead National Health Service (NHS) Trust to the Royal Free Centre for Biomedical Science. M.G.W. and J.J.H. acknowledge support provided by Cancer Research UK Award C25540/A8562.

1. Vanhaesebroeck B, Ali K, Bilancio A, Geering B, Foukas LC (2005) Signalling by PI3K isoforms: Insights from gene-targeted mice. *Trends Biochem Sci* 30:194–204.
2. Sasaki J, et al. (2005) Regulation of anaphylactic responses by phosphatidylinositol phosphate kinase type Iα. *J Exp Med* 201:859–870.
3. Wang Y, et al. (2008) Loss of PIP5KIβ demonstrates that PIP5KI isoform-specific PIP_2 synthesis is required for IP_3 formation. *Proc Natl Acad Sci USA* 105:14064–14069.
4. Di Paolo G, et al. (2004) Impaired PtdIns(4,5)P_2 synthesis in nerve terminals produces defects in synaptic vesicle trafficking. *Nature* 431:415–422.
5. Wang Y, Lian L, Golden JA, Morrisey EE, Abrams CS (2007) PIP5KIγ is required for cardiovascular and neuronal development. *Proc Natl Acad Sci USA* 104:11748–11753.
6. Balla A, Balla T (2006) Phosphatidylinositol 4-kinases: Old enzymes with emerging functions. *Trends Cell Biol* 16:351–361.
7. Chang FS, Han GS, Carman GM, Blumer KJ (2005) A WASp-binding type II phosphatidylinositol 4-kinase required for actin polymerization-driven endosome motility. *J Cell Biol* 171:133–142.
8. Han GS, Audhya A, Markley DJ, Emr SD, Carman GM (2002) The *Saccharomyces cerevisiae* LSB6 gene encodes phosphatidylinositol 4-kinase activity. *J Biol Chem* 277:47709–47718.
9. Kim K, et al. (2006) Actin-based motility during endocytosis in budding yeast. *Mol Biol Cell* 17:1354–1363.
10. Pan W, et al. (2008) Wnt3a-mediated formation of phosphatidylinositol 4,5-bisphosphate regulates LRP6 phosphorylation. *Science* 321:1350–1353.
11. Wang J, et al. (2007) PI4P promotes the recruitment of the GGA adaptor proteins to the *Trans*-Golgi network and regulates their recognition of the ubiquitin sorting signal. *Mol Biol Cell* 18:2646–2655.
12. Wang YJ, et al. (2003) Phosphatidylinositol 4 phosphate regulates targeting of clathrin adaptor AP-1 complexes to the Golgi. *Cell* 114:299–310.
13. Minogue S, et al. (2006) Phosphatidylinositol 4-kinase is required for endosomal trafficking and degradation of the EGF receptor. *J Cell Sci* 119:571–581.
14. Craige B, Salazar G, Faundez V (2008) Phosphatidylinositol-4-kinase type II alpha contains an AP-3-sorting motif and a kinase domain that are both required for endosome traffic. *Mol Biol Cell* 19:1415–1426.
15. Salinas S, Proukakis C, Crosby A, Warner TT (2008) Hereditary spastic paraplegia: Clinical features and pathogenetic mechanisms. *Lancet Neurol* 7:1127–1138.
16. Skarnes WC, et al. (2004) A public gene trap resource for mouse functional genomics. *Nat Genet* 36:543–544.
17. Guo J, et al. (2003) Phosphatidylinositol 4-kinase type IIα is responsible for the phosphatidylinositol 4-kinase activity associated with synaptic vesicles. *Proc Natl Acad Sci USA* 100:3995–4000.
18. Balla A, Tuymetova G, Barshishat M, Geiszt M, Balla T (2002) Characterization of type II phosphatidylinositol 4-kinase isoforms reveals association of the enzymes with endosomal vesicular compartments. *J Biol Chem* 277:20041–20050.
19. Seehafer SS, Pearce DA (2006) You say lipofuscin, we say ceroid: Defining autofluorescent storage material. *Neurobiol Aging* 27:576–588.
20. Jung G, et al. (2008) Molecular determinants of activation and membrane targeting of phosphoinositol 4-kinase IIbeta. *Biochem J* 409:501–509.
21. Salazar G, et al. (2009) Hermansky-Pudlak Syndrome protein complexes associate with phosphatidylinositol 4-kinase type IIα in neuronal and non-neuronal cells. *J Biol Chem* 284:1790–1802.
22. Newell-Litwa K, Seong E, Burmeister M, Faundez V (2007) Neuronal and non-neuronal functions of the AP-3 sorting machinery. *J Cell Sci* 120:531–541.
23. Ohno H (2006) Physiological roles of clathrin adaptor AP complexes: Lessons from mutant animals. *J Biochem* 139:943–948.
24. Wiedemann C, Schafer T, Burger MM, Sihra TS (1998) An essential role for a small synaptic vesicle-associated phosphatidylinositol 4-kinase in neurotransmitter release. *J Neurosci* 18:5594–5602.
25. Takamori S, et al. (2006) Molecular anatomy of a trafficking organelle. *Cell* 127:831–846.
26. Ashton AC, Ushkaryov YA (2005) Properties of synaptic vesicle pools in mature central nerve terminals. *J Biol Chem* 280:37278–37288.
27. Voglmaier SM, et al. (2006) Distinct endocytic pathways control the rate and extent of synaptic vesicle protein recycling. *Neuron* 51:71–84.
28. Khvotchev M, Sudhof TC (1998) Newly synthesized phosphatidylinositol phosphates are required for synaptic norepinephrine but not glutamate or gamma-aminobutyric acid (GABA) release. *J Biol Chem* 273:21451–21454.
29. Ferreirinha F, et al. (2004) Axonal degeneration in paraplegin-deficient mice is associated with abnormal mitochondria and impairment of axonal transport. *J Clin Invest* 113:231–242.
30. Bartlett SE, Reynolds AJ, Weible M, 2nd, Hendry IA (2002) Phosphatidylinositol kinase enzymes regulate the retrograde axonal transport of NT-3 and NT-4 in sympathetic and sensory neurons. *J Neurosci Res* 68:169–175.
31. Reynolds AJ, Heydon K, Bartlett SE, Hendry IA (1999) Evidence for phosphatidylinositol 4-kinase and actin involvement in the regulation of ^{125}I-β-nerve growth factor retrograde axonal transport. *J Neurochem* 73:87–95.
32. Hirokawa N, Takemura R (2005) Molecular motors and mechanisms of directional transport in neurons. *Nat Rev Neurosci* 6:201–214.
33. Mitne-Neto M, et al. (2007) A multi-exonic SPG4 duplication underlies sex-dependent penetrance of hereditary spastic paraplegia in a large Brazilian pedigree. *Eur J Hum Genet* 15:1276–1279.
34. Murashov AK, Islamov RR, McMurray RJ, Pak ES, Weidner DA (2004) Estrogen increases retrograde labeling of motoneurons: Evidence of a nongenomic mechanism. *Am J Physiol* 287:C320–326.
35. Martignoni M, Riano E, Rugarli EI (2008) The role of ZFYVE27/protrudin in hereditary spastic paraplegia. *Am J Hum Genet* 83:127–128; author reply 128–130.
36. Kumar S, et al. (1994) Milk composition and lactation of β-casein-deficient mice. *Proc Natl Acad Sci USA* 91:6138–6142.
37. Rogers DC, et al. (1997) Behavioral and functional analysis of mouse phenotype: SHIRPA, a proposed protocol for comprehensive phenotype assessment. *Mamm Genome* 8:711–713.
38. Schnell SA, Staines WA, Wessendorf MW (1999) Reduction of lipofuscin-like autofluorescence in fluorescently labeled tissue. *J Histochem Cytochem* 47:719–730.